Track-depth-resolved dynamics of helium excimers along 4-MeV/amu N-ion tracks in near-liquid and liquid helium

Kazuie Kimura
RIKEN (The Institute of Physical and Chemical Research), Wako Saitama 351, Japan
(Received 18 November 1991; revised manuscript received 13 August 1992)

A track scope, composed of an imaging quartz fiber and a position-sensitive photon counter, was developed. Luminescence spectra, their specific intensities dL/dx, and efficiencies dL/dE were measured as functions of the helium density and of depth along the N- and He-ion tracks in dense gas and liquid helium. Observed luminescences are limited to those due to Rydberg states of excimers, ^3d, ^3D, ^3H, and ^3J, according to Herzberg's notation. It is concluded that they are produced only by the bimolecular reaction of the lowest triplet excimer ^3a and that the excess energy of this reaction must be removed by the third body. Therefore, with increasing density of excitation, dL/dx and dL/dE are enhanced, but in an extreme case near the track termination, dL/dx is suppressed because the three-body reaction cannot find the third body except for the excimer ^3a. The appearance of an additional peak of dL/dE near the N-ion-track termination suggests the importance of additional processes such as direct excitation and charge exchange. The drastic suppression of excimer luminescences with increasing helium density is explained by instabilities of helium-excimer bubbles.

PACS number(s): 34.50.Bw, 61.80.Mk, 79.20.Nc

I. INTRODUCTION

One of the most characteristic radiation effects of heavy-ion irradiation in condensed matter is the high-density excitation of electrons in an outermost shell. In general, most of the high-energy states, such as ions and excited states of inner-shell electrons, can be converted into lower excited states of the outermost shell by Auger processes and cascade transitions. Energy deposition from a projectile ion varies along its path and it can amount to as much as 1000 eV/Å in cases of some heavy ions. As stated in Ref. [1], the effect of high-density excitation is considered to be much larger than that estimated from dE/dx, especially near the termination of the ion track; a maximum of the energy deposition per unit volume would be shifted to the track end. In addition, additional effects such as charge exchange and direct excitation, which are not included explicitly in stopping-power calculations [2,3], may be expected to become important in the region of low ionic energy near track termination. Other radiation effects characteristic in solids are also important in this region. What changes are actually caused in matter by such radiation effects and how the depth dependence along the ionic track is expressed, are important unsolved problems.

There are many historical works for measurements of the Bragg curve, for example, those done by Jesse, Forstat, and Sadauskis [4] and by Riezler and Rudoloff [5]. Their works were done for gases irradiated by He ions. On the other hand, scintillation studies on a system of thin scintillators with various ionic energies may give similar information for radiation effects [6,7]. Nowadays, it is necessary to extend studies on the Bragg curve to systems of heavy-ion projectiles and condensed-matter targets which cannot be made into a thin foil. So far, we have developed a track scope using a lens system and one composed of an imaging-fiber bundle and a position-sensitive photon counter [8–10]. We have measured track-depth-resolved luminescences on cluster and liquid helium irradiated with 4-MeV/amu N and He ions. Such luminescence measurements can inform us about depth-resolved dynamics of excited states, i.e., physicochemical primary stages for radiation effects of ions. Luminescences from ion-irradiated He, assigned to excimer luminescences, had maximum efficiencies at deeper track depths than those due to the maximum stopping power, in contrast with the usual scintillators, which show large decreases in the efficiency towards the maximum stopping power [11]. Helium is therefore a useful material for the study concerning high-density excitation in deep tracks. In addition, its simple structure and a number of spectroscopic studies (some of them are cited in Refs. [8–10]) can help us to analyze experimental data.

In this paper, based on the measurements of depth-resolved dL/dx for N-ion and α tracks, the mechanisms for the formation and suppression of excimers, the effect of the helium density and an additional peak in Bragg-type curves are discussed.

II. EXPERIMENT

The track scope was composed of a 1-m imaging-fiber bundle with a square cross section of 2×2 mm^2 where 10 000 quartz fibers were bundled (Furukawa Electronic Co., Ltd), a stainless-steel slit with a cross section of 2×0.1 mm^2 for beam aperture, a cryostat (modified CF-200, Oxford Co.), and a position-sensitive photon counter (OMA 1, Princeton Applied Research Co.). Construction of the scope is the same as the one used in Ref. [10]. The helium density was changed in a range of from 0.005 to 0.09 g/cm^3 by adjusting pressure at temperature around 8 K. Helium with a density greater than about 0.05 g/cm^3

was in liquid phase at the above pressure and temperature. Thus the track lengths could be changed by adjustment of the helium density. Extension of the track lengths is important for the track-depth-resolved measurements, since the track length of few MeV ions is too short in usual liquid and solid targets (less than 10 μm) to be resolved.

Helium was irradiated with a N- or He-ion beam with a cross section of 0.1×2 mm^2, which formed a bundle of ion tracks of the same cross section. The end of the imaging fiber was close to the plane of ion tracks (0.1 mm). This end could slide perpendicularly to the beam plane by a remote control system to get the maximum beam flow, and also slide laterally along the track depth to observe the full track, up to the maximum of 6.3 mm (see Fig. 1 of Ref. [10]). This end and the other light-outlet end were vacuum sealed to each other. The track image emitted from the light-outlet end of the fiber was focused on the photoplate of the OMA using a lens system, which gave a track-depth-resolved specific luminescence dL/dx vs depth. By setting the outlet end close to the monochromator slit, i.e., by measuring a slice of the image by using the OMA, the luminescence spectrum at a given track depth could be obtained. Measurements made while sliding the fiber to the slit give a depth-resolved luminescence spectrum. A measurement using a photomultiplier instead of the OMA gives a luminescence decay at a given wavelength and at a given track depth. By measuring while sliding the fiber to the slit and scanning the wavelength, depth-resolved spectral decay can be obtained. The resolution of the depth was estimated at least to be 0.02 mm.

Ions were accelerated by the 160-cm cyclotron of our institute RIKEN to 4.656 MeV, for example. The width of each beam bunch was 3 ns and its period was 120 ns. The number of ions irradiated were counted by using a detector composed of thin carbon foils [10]. A correction of the ion energy was done, since the ionic energy was degraded by carbon foils, an aluminum foil as a window, and target helium from the window to the front edge of the fiber; e.g., it was 3.687 MeV in the case of helium with a density of 0.0316 g/cm^3.

Since we have no density data of helium being available to present extreme conditions, the helium density was estimated from Northcliffe's tables [2] for ranges (density $\times$track length) vs energies. As ionic energies and track lengths are given experimentally, the value of the density can be calculated from Northcliffe's table. The density estimated seems to be reasonable, as it was compared with the value extrapolated from NBS table [12]. Although this estimation may not give precise values, it would be self-consistent within analysis of experimental data in this work, since the quantities such as stopping power, range, energy, and velocity were also calculated using Northcliffe's table.

III. RESULTS AND DISCUSSIONS

A. Track-depth-resolved specific luminescence dL/dx

Figure 1 shows track-depth-resolved specific luminescence dL/dx, observed at various helium densities. The

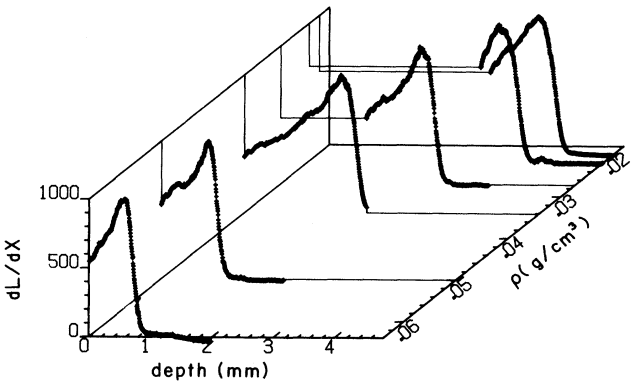

FIG. 1. Specific luminescence of UV and visible light, dL/dx, vs the depth of N-ion track and its helium-density dependence. All the curves are illustrated in equal maximum heights. The ordinate is expressed in an arbitrary unit.

dL/dx is a sum of luminescences in a wavelength region from 3000 to 8000 Å. Although this figure illustrates all the curves with equal heights, in fact dL/dx were strongly dependent on helium density, as shown in next section. The dependence of dL/dx on track depth was scarcely dependent on wavelengths, while the luminescence intensity was largely dependent on wavelengths, which is also discussed in next section.

1. Spectral assignment and dependence on helium density

Figures 2(a) and 2(b) show luminescence spectra measured at different helium densities and track depths. Only four peaks can be recognized in the figures. The assignments of these peaks and why the number of peaks observable is so small will be discussed in an earlier part of this section and then a formation mechanism for origins of luminescences will be discussed. A number of atomic-luminescence lines about helium gas at low pressure have been observed by many investigators by means of discharge. At higher pressures, more than a few tens Torr, excimer luminescence appears instead of atomic luminescence. Almost all excimer luminescences are assigned as transitions between Rydberg states. Energy levels of excimers, which are based on data quoted in a book by Huber and Herzbeg [13], are shown schematically in Fig. 3. Lower-case characters stand for triplet excimers and capitals for singlet excimers. With increasing pressure, the peak wavelengths of luminescences are found to be scarcely shifted, which is explained because an excimer can rotate freely in a bubble (or a cavity) surrounding the excimer. Therefore one can assign spectral peaks easily. The present four peaks observed at 6396, 6590, 7040, and 7260 Å are assigned to be due to ^3d-^3b, ^1D-^1B, ^1J-^1C, and ^1H-^1C.

Luminescence intensities of helium excimers were influenced largely by the helium density. With increasing density, the bubble radius is reduced so that Rydberg states of large radius cannot exist. Namely, Rydberg states having the larger principal quantum numbers are more unstable. This results in suppression of luminescences and a number of peaks are quenched in order of

the radius of the excimer. In case of a density of 6 mg/cm^3, only luminescence peaks due to the transitions united with solid lines shown in Fig. 3 were observable (see Refs. [8,9]). Thus the present observation of only four peaks can be explained by the instability of the bubble at high densities of helium. No further eliminations of peak number occurred even in the liquid phase, although their intensities are decreased.

The density dependences of specific luminescence dL/dx of ^3d-^3b are shown in Fig. 4. The curves consist of an increasing part, a peak at about 0.01 g/cm^3, and a rapidly decreasing part. The increasing part of the curve will be explained in the next section. The decreasing part should be due to the aforementioned mechanism, namely, by instabilization of Rydberg states by reducing radius of the bubble or its instability. The stability of the bubble is considered to depend on whether the total energy is lower or higher than the energy of the quasifree state. The total energy should be approximated as a sum of energies of electron-He^+ core, electron-liquid, He^+ core-liquid, bubble, and attractive dispersion, similar to a bubble of an excited atom [14]. As the situation is similar to the electron bubble in helium except for attractive dispersion in this case, the discussion for the stability of the electron bubble is applicable qualitatively to the present case.

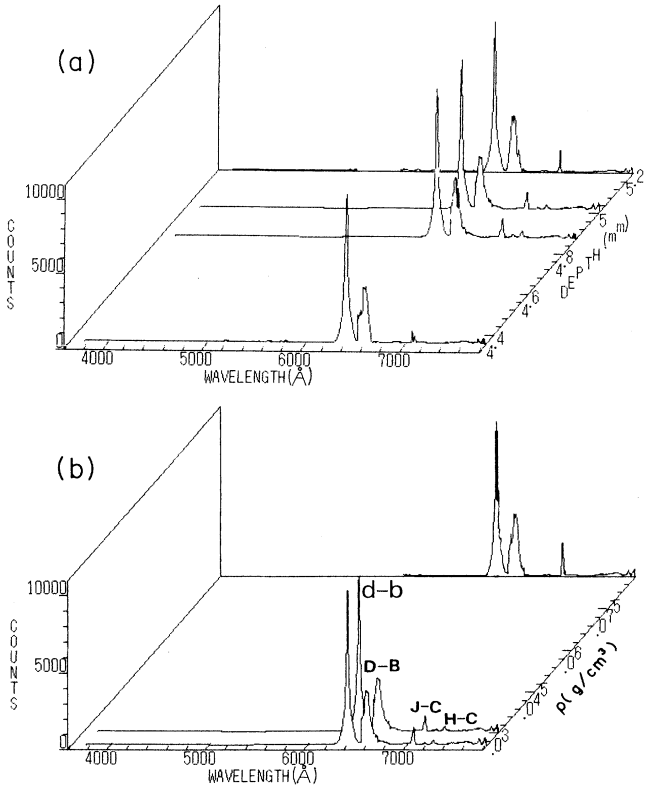

FIG. 2. Track depth and density-dependent luminescence spectra of N-ion-irradiated helium. (a) Track-depth-dependent spectra at the helium density of 0.025 52 g/cm^3. (b) Density-dependent spectra at track depths from 0.8 to 5.3 mm. All the spectra are illustrated in equal heights for ^3d-^3b and their intensities at larger wavelengths than 6500 Å are enlarged ten times.

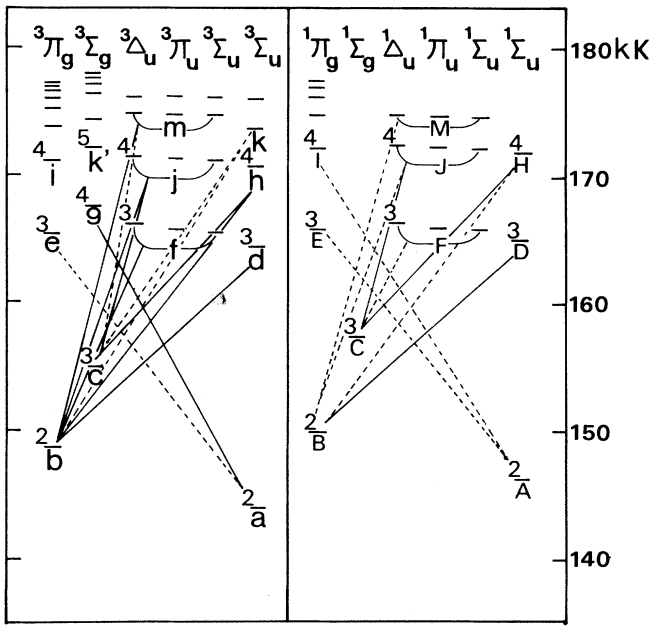

FIG. 3. Energy-level diagram of helium excimers. Term values are quoted from Ref. [13]. Capital and lower-case letters stand for singlet and triplet states, respectively. The levels united by solid lines shows transitions observed at the density of 6 mg/cm^3 (Ref. [8]).

Webman and Jortner calculated the stability of the electron bubble and showed to a large extent the instabilization with increasing pressure [15]. Although our experimental condition (pressure larger than 600 Torr at about 8 K) does not fit satisfactorily to their conditions, ours seems near one of their conditions; that at pressure higher than 10 atm at 20.4 K. Thus the present large decrease in specific luminescence may be explained by the rapid instabilization of the bubble with increasing density.

An intensity ratio among the four luminescence peaks was scarcely invariant to the variation of both the density

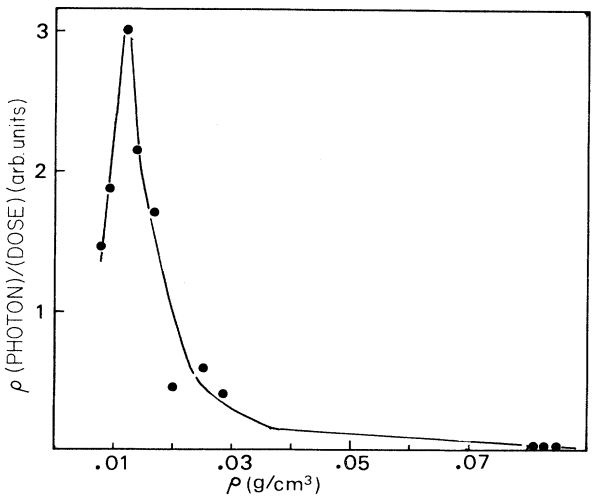

FIG. 4. Dose- and density-normalized dL/dx vs density. The data of dL/dx are those at a track depth of 0 mm.

and the depth of track, as shown in Figs. 2(a) and 2(b). This result suggests that the excimers observed are formed by the same formation mechanism. A characteristic bimolecular reaction is known in dense helium,

$$^3a + {}^3a \longrightarrow {}^3d\ ,\ {}^1D\ ,\ {}^1J\ ,\ {}^1H\ ,\ \text{and}\ {}^1A\ . \qquad (1)$$

If the rate equation of this reaction is solved, it can be derived that the inverse of the square root of excimer luminescence increases linearly with time. This reaction was ascertained by agreement between the requirement aforementioned and experimental plots [8,9,16]. The invariance of the intensity ratio can be explained completely by considering that all excimers observable in the present condition can be formed by this reaction. The higher-level Rydberg states which may be formed directly at the primary stage are considered to be relaxed to excimers ^3a or ^1A nonradiatively.

2. *Excitation-density dependence of dL/dx*

Figure 1 shows that each curve of dL/dx vs track depth has a peak maximum which appears independently of helium densities. The peak appears even at high density where dL/dx is suppressed considerably by the instabilization of the bubble. This suggests that there are some mechanisms apart from the effect of helium density. The effect excluding that of helium density in Fig. 1 can be expressed by the plot of dL/dx as a function of the range whose dimension is [length $\times$ g/cm^3]. The result is given in Fig. 5. The peaks appear to shift towards the larger (residual) rangle with increasing density of helium. Such shifts mean that the range is not a good parameter to depict the curves of dL/dx vs track depth. Also, it was checked in the same way that stopping power and ionic energy were not good parameters.

Next, dL/dx was plotted as a function of energy deposition per unit volume (the excitation density), as shown in Fig. 6. The relative excitation density was estimated in the same way as done previously [10]. Now, peaks coincide at a given excitation density, and hence formation

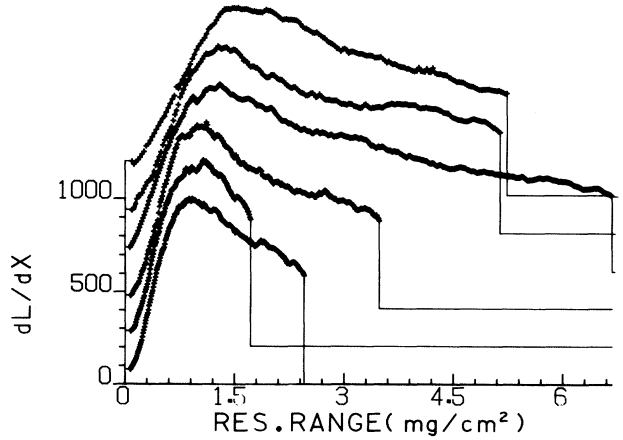

FIG. 5. dL/dx vs N-ion residual range at various helium densities. The figure was obtained by conversion of the track lengths in Fig. 1 into the ranges using Northcliffe's table [2]; the densities are, from top to bottom, 0.02, 0.0219, 0.0273, 0.0342, 0.0498, and 0.0638 g/cm^3.

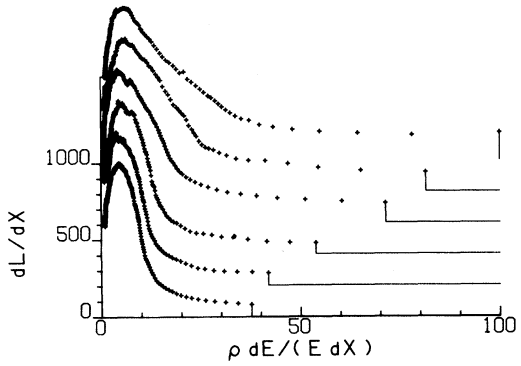

FIG. 6. dL/dx vs excitation density induced by N ions and its helium-density dependence. The excitation density was assumed to be described by (helium density ρ)$\times$(dE/dx)$/E$ [10]. Both ordinate and abscissa are in arbitrary units. The densities are the same as those in Fig. 5.

and suppression of excimer luminescence should be expressed by the excitation density. The increase in dL/dx with increasing excitation density (namely, with deeper propagation of ions) can be explained easily by enhancement of the regeneration reaction (1) with increasing concentration of ^3a. With further increasing excitation density, dL/dx attains a peak and then decreases rapidly. The suppressing mechanism wherein upper-level excimers such as ^3d are quenched by collisions with any of excimers z may be the first one to be checked. If this quenching reaction competes with radiative decay of the excimer ^3d, then

$$^3d + z \longrightarrow \text{quenching}\ , \qquad (2)$$

$$^3d \longrightarrow {}^3b + \text{photon}\ . \qquad (3)$$

As a candidate of z, excimers other than ^3a cannot be considered because it has an extremely long lifetime and high stationary concentration [8–10,16]. A rate of production of ^3d can be expressed by the following equation:

$$\frac{d[^3d]}{dt} = k_1[^3a]^2/2 - (k_2[^3a] + k_3)[^3d]\ , \qquad (4)$$

where $k_i (i = 1,2,3)$ stands for the rate constant due to reaction (1), (2), or (3). Since the state ^3d disappears too fast to be stored [8,9], $d[^3d]/dt$ can be approximated to be 0. Therefore we obtain

$$[^3d] = k_1[^3a]^2/2(k_2[^3a] + k_3)\ . \qquad (5)$$

Instantaneous luminescence $I(t)$ can be expressed as $k_3[^3d]$;

$$I(t) = k_3 k_1[^3a]^2/2(k_2[^3a] + k_3)\ . \qquad (6)$$

In order to explain the decreases in dL/dx shown in Fig. 6, the derivative of $I(t)$ for the excitation density should be negative. The derivative may be replaced with $dI(t)/d[^3a]$, since the excitation density may practically be replaced by a concentration of ^3a, $[^3a]$. The condition $dI(t)/d[^3a] < 0$ yields the relation $k_2[^3a] + k_3 < 0$. Since this is impossible, it is concluded that the process (2) can-

not explain experimental result. This discussion should be applicable to excimers other than the excimer ^3d. It has also been deduced previously that excimer reactions such as (2) are not effective quenching mechanisms in helium [8,9]. Therefore a different type of decreasing mechanisms must be considered.

The energy balance of reaction (1) is as follows:

$$\underset{17.86\ \text{eV}}{^3a} + \underset{17.86\ \text{eV}}{^3a} \longrightarrow \underset{20.39\ \text{eV}}{^3d} + \underset{0\ \text{eV},}{2\text{He}} \quad E_{\text{IP}}=22.223\ \text{eV}$$

The energy difference between the right-hand side and the left-hand side is as large as 15.32 eV. This excess energy is too large to transfer to two helium atoms as the translational energy: since the reaction of two ^3a has a large excess energy of 13.22 eV beyond the ionizing position E_{IP}, the reaction should be led to the autoionizing process rather than to the formation of the excimer ^3d. Therefore it should be reasonable that reaction (1) proceeds in fact as a third-body reaction. Then excess energy can be removed in the same way that helium excimers are formed by three-body collisions.

$$^3a + {}^3a + \text{He} \longrightarrow {}^3d + X + \text{He} \ . \tag{1'}$$

Under the high-density excitation near the track termination, the concentration of ^3a may be comparable with that of He. Namely, the following nonradiative reaction become important and can compete with reaction (1'),

$$^3a + {}^3a + {}^3a \longrightarrow \text{dissociative} \ . \tag{7}$$

Now it is checked whether the three competing reactions (1'), (3), and (7) can explain the decrease in dL/dx with increasing density of excitation. Similar consideration to the derivation of Eq. (5) leads to the following equation:

$$[^3d]=k_1[^3a]^2[\text{He}]/2k_3 \ . \tag{8}$$

Here, [He] is not constant but dependent on $[^3a]$. When there exist N_a molecules of ^3a and N_h atoms of He in a volume V, V can be expressed by a sum of volumes of $N_a v_a$ and $N_h m v_a$, where v_a and m stand for the volume occupied by an ^3a and a ratio of the volume occupied by a He atom to v_a. Consequently, a concentration of He, [He], and instantaneous luminescence $I(t)$ can be described as

$$\begin{aligned} &[\text{He}]=N_h/V=(1/v_a-N_a/V)/m \ , \\ &I(t)=k_1[^3a]^2(1/v_a-[^3a])/2m \ . \end{aligned} \tag{9}$$

The criteria $dI(t)/d[^3a]<0$ leads to

$$1/2v_a<[^3a] \ .$$

This relation means that dL/dx decreases when a concentration of ^3a exceeds half of the concentration when the space V is filled only by ^3a. Reaction (7) can therefore explain the decrease in dL/dx near the track termination.

The aforementioned effect of high-density excitation may also suppress the formation of excimers in earlier stages. Excimers are formed by the three-body reactions:

$$\text{He}^* + 2\text{He} \longrightarrow \text{excimer} + \text{He} \tag{10}$$

20.97 eV (the lowest triplet) $E_{\text{IP}}=24.58$ eV

or

$$\text{He}^+ + 2\text{He} + e \longrightarrow \text{excimer} + \text{He} \ . \tag{11}$$

If He^* or He^+ cannot find 2He, an excimer cannot be formed. This may be also a mechanism for the decrease in dL/dx.

B. Depth-resolved dL/dE

As Fig. 6 shows, dL/dx has a tail followed by the peak with propagation of the ions. This trailing was emphasized in a plot of the luminescence efficiency dL/dE, since dL/dE was calculated by dividing dL/dx with dE/dx, which is proportional to the particle velocity. Figure 7 shows dL/dE as a function of excitation density with various helium densities. The dL/dE has an increasing part and the second peak marked by the arrows at deep penetration. Both phenomena, an increase and additional peak in dL/dE, have not been found in usual scintillators whose dL/dE decrease rapidly towards the maximum dE/dx [11]. An increase in dL/dE can be explained by reaction (1), since nonradiative ^3a is converted into radiative excimers by this reaction. As for the additional peak, the peak shifts with the helium density, which implies that the peaking cannot be expressed by the excitation density. As shown in Fig. 8, the peaks are, however, coincided at the velocity of about 4×10^8 cm/s by plotting dL/dE with the ionic velocity. By contrast, α-irradiation showed a negligibly small peak at the termination, as shown in Fig. 9.

These results imply that the ratio of the luminescence yield to the average excitation energy in Voltz's equation [17] cannot be constant near the track termination but the average excitation energy decreases or a luminescence yield increases. Now we will discuss additional excitation processes which are not usually taken into account in calculations of stopping power. Such processes are charge-exchange processes and direct excitations which can produce triplet states directly. Considering that dL/dE

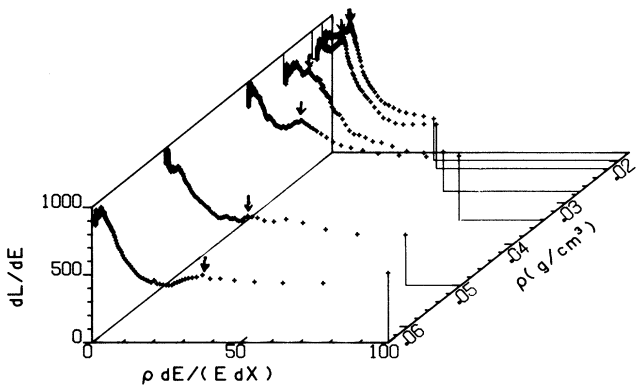

FIG. 7. dL/dE vs excitation density by N ions and its helium-density dependence. Arrows show the second peaks. Both ordinate and abscissa are in arbitrary units.

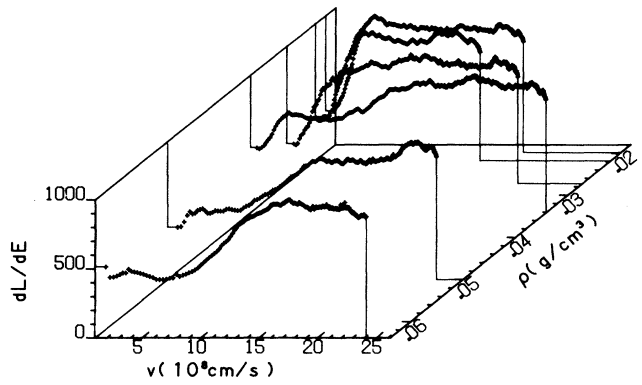

FIG. 8. dL/dE vs velocities of N ions and its helium-density dependence.

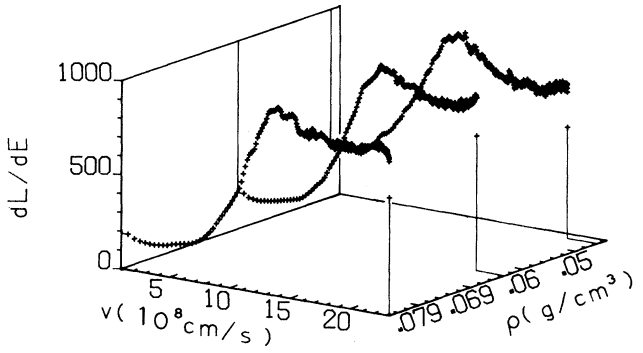

FIG. 9. dL/dE vs velocities of α particles and its helium-density dependence.

peaks are coincided at slow ionic velocity of about 4×10^8 cm/s and that this velocity is only a little faster than that of a $1S$ orbital electron of He (3×10^8 cm/s), charge-exchange processes caused by the formation of instantaneous molecular orbital [18] seems to occur easily. Also, direct formation of triplets may occur. According to Platzmann [19], when He is irradiated by electrons, $2\,^3P$ and $2\,^1P$ atomic states are formed with a similar yield, and each yield has a peak at the electron energy of 30 eV, where ionization no longer occurs. The electron velocity corresponding to this peak is nearly the same as those due to the dL/dE peaks in Fig. 8. The above two additional processes can cause an increase in dL/dE.

ACKNOWLEDGMENT

The author is indebted to many former students of Chuo University and Professor S. Sonoike. He also wishes to thank Professor T. Watanabe (International Christian University) and Dr. S. Kravis (STA fellow of RIKEN) for their helpful discussions and critical reading of the draft.

[1] K. Kimura, T. Matsuyama, and H. Kumagai, Radiat. Phys. Chem. **34**, 575 (1989).
[2] L. C. Northcliffe and R. F. Schilling, *Nuclear Data Tables* (Academic, New York, 1970).
[3] J. F. Ziegler, in *The Stopping and Ranges of Ions in Matter,* edited by J. F. Ziegler (Pergamon, New York 1980).
[4] W. P. Jesse, H. Forstat, and J. Sadauskis, Phys. Rev. **77**, 782 (1950).
[5] W. Riezler and A. Rudoloff, Ann. Phys. (Leipzig) **6**, 224 (1955).
[6] S. P. Ahlen, Rev. Mod. Phys. **52**, 121 (1980).
[7] F. D. Becchetti, C. E. Thorn, and M. J. Levine, Nucl. Instrum. Methods. **138**, 93 (1976).
[8] K. Kimura, J. Chem. Phys. **84**, 2002 (1986).
[9] K. Kimura, J. Chem. Phys. **84**, 2010 (1986).
[10] K. Kimura, Nucl. Instrum. Methods. **B53**, 301 (1991).
[11] S. P. Ahlen, Rev. Mod. Phys. **52**, 121 (1980).
[12] *Properties of Materials at Low Temperature (Phase 1), A Compendium,* edited by V. J. Johnson (Pergamon, New York, 1961).
[13] K. P. Huber and G. Herzberg, *Molecular Spectra and Molecular Structure. IV. Constants of Diatomic Molecules* (Van Nostrand Reinhold, New York, 1978).
[14] A. P. Hickman and N. F. Lane, Phys. Rev. Lett. **26**, 1216 (1971).
[15] I. Webman and J. Jortner, in *Electrons in Fluids,* edited by J. Jortner and N. R. Kestner (Springer, Berlin, 1973), p. 423.
[16] J. W. Keto, F. J. Soley, M. Stockton, and W. A. Fitzsimmons, Phys. Rev. A **10**, 887 (1974).
[17] R. Voltz, J. Lopes da Silva, G. Laustriat, and A. Coche, J. Chem. Phys. **45**, 3306 (1966).
[18] U. Fano and W. Lichten, Phys. Rev. Lett. **14**, 627 (1965).
[19] L. Platzman, Int. J. Appl. Radiat. Isot. **10**, 116 (1961).